

## Potentiometric Study and Biological Activity of Some Metal Ion Complexes of Polyvinyl Alcohol (PVA).

Wafaa M. Hosny\*, Perihan. A. Khalaf-Alaa

Chemistry Department, Faculty of Science, Cairo University, Giza, Egypt

\*E-mail: [dr\\_wafaa1960@yahoo.co.uk](mailto:dr_wafaa1960@yahoo.co.uk)

Received: 13 October 2012 / Accepted: 26 November 2012 / Published: 1 January 2013

---

The acid-base equilibrium of polyvinyl alcohol (PVA) is investigated. The stability constant values of the binary complexes between PVA and metal ions Cu(II), Co(II), Ni(II) and Zn(II) formed in solution were investigated potentiometrically. The relationships between the properties of the studied central metal ions as ionic radius, electronegativity, atomic number, and ionization potential of the formed complexes were investigated and give information about the nature of chemical bonding in complexes and make possible the calculation of unknown stability constants. Cu<sup>II</sup> and Ni<sup>II</sup> complexes with PVA are isolated as solid complexes and characterized by chemical and physical methods, and their general formula [ML.nH<sub>2</sub>O]2H<sub>2</sub>O, where M = Cu<sup>II</sup> and Ni<sup>II</sup>, L = PVA, and n = 2 and 4 for Cu<sup>II</sup> and Ni<sup>II</sup> respectively. The ligand and their metal chelates have been screened for their antimicrobial activities using the disc diffusion method against the selected bacteria and fungi.

---

**Keywords:** Polyvinyl alcohol(PVA); Metal complexes; Potentiometry; IR spectra; Antimicrobial activities

### 1. INTRODUCTION

Polymer complexes have been given a great deal of attention in recent years [1-3]. Polyvinyl alcohol (ethanol homopolymer) which considered as moderate adhesive is a water – soluble resin. PVA is a polymer with exceptional properties such as water solubility, biodegradability, biocompatibility, non-toxicity and non-carcinogenicity that possesses the capability to form hydrogels by chemical or physical methods[4–6]. Its fields of applicability were widely broadened during the later years due to the development of medicine.

In this paper we used the hydrolyzed [7] (98.9%) PVA with weight averaged molecular weight Mw= 27,000 ( the number averaged molecular weight Mn=14, 000) was purchased from Aldrich Chemical Company; it is clear that the use of transition action of our previous studies of the metal

complexes of polymer[8-11], it seems interesting to study the coordination properties of PVA and its metal complexes. In this investigation, we report a quantitative study of the acid base equilibrium of PVA, as well as the binary complex formation equilibria with Cu(II), Co(II), Ni(II) and Zn(II)<sup>2+</sup>, the concentration distributions of the complexes are evaluated. We have also studied the effect of metal ion properties on the log  $K_1$  values of the binary metal complexes. The solid complexes with the metal ions Cu(II), and Ni(II) are synthesized and characterized by the physicochemical method and biological activity. This work is also extended to present some correlations between the thermodynamic functions and some of well-known properties of the metal ions. Such work may help to explain the nature and driving forces for the interactions occurring in biological systems, such as metal-protein and metal-nucleic acid interactions.

## 2. EXPERIMENTAL

### 2.1. Materials and reagents

PVA (average  $M_w$ : 27000, Aldrich makes). The metal salts used are  $\text{CuCl}_2 \cdot 2\text{H}_2\text{O}$ ,  $\text{NiCl}_2 \cdot 6\text{H}_2\text{O}$ ,  $\text{CoCl}_2 \cdot 6\text{H}_2\text{O}$ ,  $\text{ZnCl}_2 \cdot 2\text{H}_2\text{O}$ , obtained from Sigma Chem. Co, UK. Metal salt solutions were prepared and standardized as described previously[12].

### 2.2. Synthesis of the binary metal complexes

Cu(II) and Ni(II) complexes of PVA were prepared in the ratio 1:1 (metal: ligand), by direct mixing of 0.5 mmol of metal salt, 0.5 mmol of ligand in the smallest quantity of bi-distilled water. The mixture was refluxed for 1-3 h, then they form solid complexes. The latter were separated by filtration, washed with ethanol and finally with diethyl ether. The analytical data are given in Table 1.

**Table 1.** Analytical and physical data for prepared metal salts.

| Compound empirical formula   | M. Wt. | Color      | $\mu$ (B. M.) | $\Delta M$ ( $\Omega^{-1}\text{cm}^2\text{mol}^{-1}$ ) | M.P. $^{\circ}\text{C}$ | Yield % | Found(Calcd.) %  |                |
|--|--------|------------|---------------|--|-------------------------|---------|------------------|----------------|
|  |        |            |               |  |                         |         | C (C)            | H (H)          |
| $[\text{Cu}(\text{C}_3\text{H}_4\text{O}_2)_2\text{H}_2\text{O}]2\text{H}_2\text{O}$ | 207.5  | Dark green | 1.95          | 21.0   | >210                    | 85%     | 17.00<br>(17.30) | 5.66<br>(5.70) |
| $[\text{Ni}(\text{C}_3\text{H}_4\text{O}_2)_4\text{H}_2\text{O}]2\text{H}_2\text{O}$ | 238.7  | Deep green | 3.75          | 22.8   | >200                    | 90%     | 14.99<br>(15.08) | 6.68<br>(6.70) |

### 2.3. Biological activity

Antimicrobial activity of the tested samples was determined using a modified Kirby–Bauer disc diffusion method[13]. The antibacterial activities were done by using gram +ve organisms (Staphylococcus aureus and Bacillus subtilis) and gram -ve organisms (Escherichia coli and

*Pseudomonas aeruginosa*). These bacterial strains were chosen as they are known human pathogens. Briefly, 100  $\mu\text{l}$  of the test bacteria were grown in 10 ml of fresh media until they reached a count of approximately 10<sup>8</sup> cells/ml or 10<sup>5</sup> cells/ml for fungi[14]. Hundred microliters of microbial suspension was spread onto agar plates corresponding to the broth in which they were maintained. Isolated colonies of each organism that might be playing a pathogenic role should be selected from primary agar plates and tested for susceptibility by disc diffusion method of the National Committee for Clinical Laboratory Standards (NCCLS)[15]. Among the available media available, NCCLS recommends Muller-Hinton agar due to: it results in good batch-to-batch reproducibility. Plates inoculated with Gram (+) bacteria as *S. aureus*, *B. subtilis*; Gram (-) bacteria as *E. coli*, *P. aeruginosa*, they were incubated at 35–37 °C for 24–48 h and fungi as *Aspergillus flavus* and *Candida albicans* incubated at 30 °C for 24–48 h and then the diameters of inhibition zones were measured in millimeters[13-14]. Standard discs of Ampicillin (Antibacterial agent), Amphotericin B (Antifungal agent) served as positive controls for antimicrobial activity but filter discs impregnated with 10  $\mu\text{l}$  of solvent were used as a negative control. The solution in different concentrations (mg/ml) of each compound (free ligand, metal complexes and standard drug) in DMSO was prepared for testing against spore germination. The agar used is Muller-Hinton agar that is rigorously tested for composition and pH. Further the depth of the agar in the plate is a factor to be considered in the disc diffusion method. This method is well documented and standard zones of inhibition have been determined for susceptible and resistant values. When a filter paper disc impregnated with a tested chemical is placed on agar, the chemical will diffuse from the disc into the agar. This diffusion will place the chemical in the agar only around the disc. The solubility of the chemical and its molecular size will determine the size of the area of chemical infiltration around the disc. If an organism is placed on the agar, it will not grow in the area around the disc if it is susceptible to the chemical. This area of no growth around the disc is known as a “Zone of inhibition” or “Clear Zone”. For the disc diffusion, the zone diameters were measured with slipping calipers of the (NCCLS)<sup>[15]</sup>. Agar-based methods such as E-test and disk diffusion can be good alternatives because they are simpler and faster than the broth-based methods[16-17].

## 2.4. Apparatus and measuring techniques

### 2.4.1. Instruments, apparatus and measuring techniques

Potentiometric measurements were made using a Metrohm 751 Titrino. The titroprocessor and electrode were calibrated with standard buffer solutions, prepared according to NBS specifications<sup>[12]</sup> at  $25 \pm 0.1^\circ\text{C}$  and  $I = 0.1 \text{ mol dm}^{-3}$ , potassium hydrogen phthalate (pH 4.008) and a mixture of  $\text{KH}_2\text{PO}_4$  and  $\text{Na}_2\text{HPO}_4$  (pH 6.865). A  $(0.10 \text{ mol dm}^{-3})$  standard acid solution was titrated with a standard base  $(0.10 \text{ mol dm}^{-3})$  to convert the pH meter reading into hydrogen ion concentration. The pH values were plotted against  $\text{p}[\text{H}]$ , where the relation  $\text{pH} - \text{p}[\text{H}] = 0.5$  was observed for all the titration data. A  $\text{p}K_w$  value of 13.997[18] was used to calculate the  $[\text{OH}^-]$ . The titrations were performed in a thermostated titration vessel equipped with a magnetic stirring system, under purified  $\text{N}_2$  atmosphere using 0.05 M NaOH as titrant. The titrations were performed at a constant ionic strength of  $0.1 \text{ mol. dm}^{-3}$  ( $\text{NaNO}_3$ ). The micro chemical analysis of the separated solid complexes for C, H and N was

performed in the micro analytical center, Cairo University. The analyses were performed twice to check the accuracy of the analytical data. IR spectra were measured on an 80486-pc FTIR Shimadzu spectrophotometer using KBr pellets. The magnetic susceptibility measurements for the complexes were determined by the Gouy balance using  $\text{Hg}[\text{Co}(\text{NCS})_4]$  as a calibrant at room temperature [19]. The acid dissociation constants of the ligand were determined by titrating a 40 ml of ligand solution ( $1.25 \times 10^{-3} \text{ mol dm}^{-3}$ ). The formation constants of the complexes were determined by titrating 40 mL of the solution containing metal ion ( $1.25 \times 10^{-4} \text{ mol dm}^{-3}$ ) and ligand ( $1.25 \times 10^{-3} \text{ mol dm}^{-3}$ ). The stability constant values were calculated by using the computer program MINQUAD-75<sup>[20]</sup>. Various possible composition models were tried to calculate the stoichiometry and stability constants of the system studied. The model selected was that which gave the best statistical fit as described before [20]. The experimental titration data points were compared with the theoretical curve calculated from the acid dissociation constant values of the ligand and the formation constants of their complexes, in order to check the validity of the selected model. Table 3 lists the stability constants together with their standard deviations and the sum of the squares of the residuals derived from the MINQUAD output. The speciation diagrams were obtained using the program SPECIES [21].

#### 2.4.2. Spectrophotometric measurements

A spectrophotometric investigation of the binary and ternary Cu(II) complexes with PVA was performed by scanning the visible spectra of solution mixtures (A and B). Under the prevailing experimental conditions and after neutralization of the released hydrogen ions, associated with complex formation, it is assumed that the complexes have been completely formed. The samples utilized for spectrophotometric measurements were prepared as follows:

A-  $1 \text{ cm}^3$  ( $0.01 \text{ Mol dm}^{-3}$ ) Cu(II) ion

B-  $1 \text{ cm}^3$  ( $0.01 \text{ Mol dm}^{-3}$ ) Cu(II) ion +  $2 \text{ cm}^3$  ( $0.01 \text{ Mol dm}^{-3}$ ) PVA + amount of base required to neutralize the  $\text{H}^+$  liberated from complex formation. In each case the final volume was brought to  $10 \text{ cm}^3$  by the addition of deionized water, the ionic strength is kept constant at  $0.1 \text{ mol dm}^{-3} \text{ NaNO}_3$ .

### 3. RESULTS AND DISCUSSION

#### 3.1. Acid base equilibrium of polyvinyl alcohol

PVA is prepared in one equivalent of  $\text{HNO}_3$  solution to allow pronation of the hydroxyl group and formation of HL species, which acts as a monoprotic acid according to the following equilibrium



Generally, the following equilibrium could be used to describe the cumulative (overall) formation constant  $\beta_{pqr}$  of the species.



$$\beta_{pqr} = \frac{[MP_p L_q H_r]}{[M]^p [L]^q [H]^{aq}} \quad (3)$$

(Charges on individual species are omitted for simplicity).

Here, we have no metal complex formation ( $p=0$ ), then only protonation of PVA according to Eq. 1 will occur.

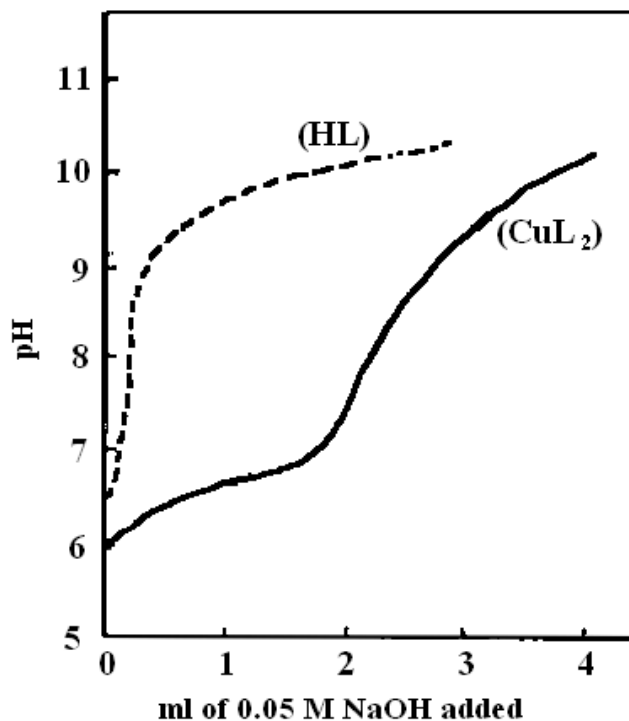


Figure. 1. Potentiometric titration curves for PVA (HL) and  $CuL_2$  systems

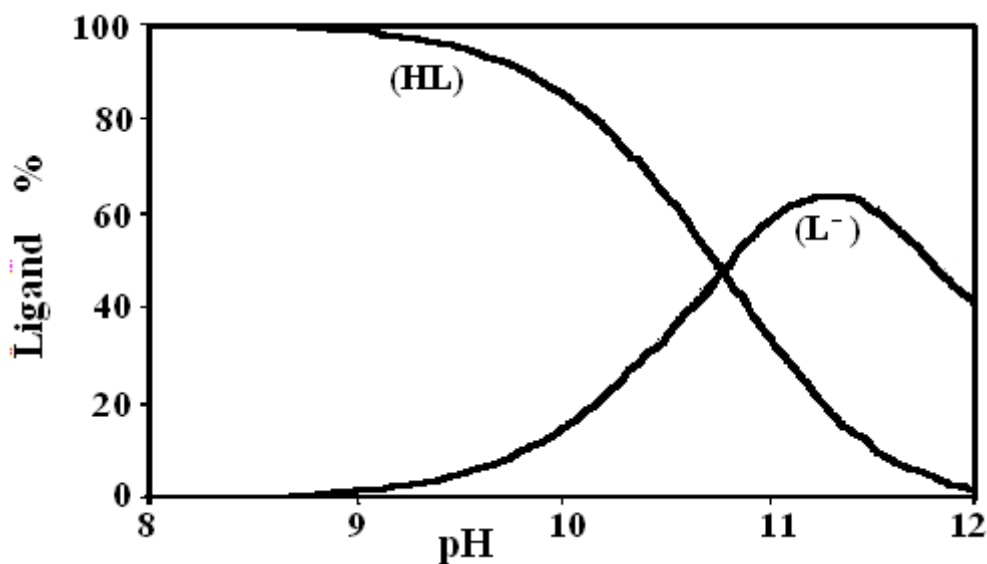


Figure 2. Concentration distribution diagram of the various forms of HL.

Fig. 1, shows the potentiometric titration of PVA with a base. From the Fig, it is clear that there is a first deprotonation stage of the hydroxyl group with a peak value of 10.67 ( $pK_a = \log\beta_{011}$ ). Fig. 2, shows the concentration distribution diagram of PVA. At pH 8, the protonated species of the ligand, HL, appears, and on increasing pH the concentration of HL decreases and the deprotonated species  $L^-$  starts to form and reaches a maximum concentration of 60 % at pH 11. The  $L^-$  species is predominating in the physiological pH range.

### 3.2. Binary complexes involving PVA with the metal ions Cu(II), Ni(II), Co(II) and Zn(II)

Table 2 lists the stoichiometry and stability constants of the binary complexes formed with PVA together with the proton association constants of PVA. The metal ions with the ligand are titrated potentiometrically with NaOH. A displacement was observed in the metal-ligand titration curves compared to the ligand titration curve. This indicated the release of protons upon complex formation. The potentiometric titration data of the binary complex formation equilibria were fitted to various models. The titration data fit satisfactory with the formation of the deprotonated species 110 (Metal: ligand 1:1), and the deprotonated species 120 (Metal: ligand 1:2).

**Table 2.** Stability constants of PVA complexes where <sup>a</sup>p, q and r are the stoichiometric coefficients corresponding to metal(II), PVA and  $H^+$  respectively. <sup>b</sup> standard deviation are given in parentheses. <sup>c</sup> sum of square of residuals

| System        | p | q | r | $\log\beta^b$ | $S^c$                 |
|---------------|---|---|---|---------------|-----------------------|
| <b>PVA</b>    | 0 | 1 | 1 | 10.67(0.01)   | $5.10 \times 10^{-7}$ |
| <b>Cu-PVA</b> | 1 | 1 | 0 | 8.07(0.02)    | $5.70 \times 10^{-8}$ |
|               | 1 | 2 | 0 | 15.93(0.03)   |                       |
| <b>Co-PVA</b> | 1 | 1 | 0 | 5.67(0.02)    | $3.90 \times 10^{-8}$ |
|               | 1 | 2 | 0 | 11.06(0.05)   |                       |
| <b>Ni-PVA</b> | 1 | 1 | 0 | 6.21(0.01)    | $4.80 \times 10^{-7}$ |
|               | 1 | 2 | 0 | 11.82(0.03)   |                       |
| <b>Zn-PVA</b> | 1 | 1 | 0 | 6.97(0.02)    | $6.70 \times 10^{-9}$ |
|               | 1 | 2 | 0 | 13.57(0.04)   |                       |

Comparison of the potentiometric titration data with the theoretically simulated curve of the protonation constant of HL and the formation constants of the formed binary complexes in solution was carried out in order to test the validity of the complex formation model selected. The concentration distribution of the various species formed in solution was estimated in order to provide a useful picture of metal ion binding. Fig. 3 represents the speciation diagram of the binary Cu(II) complex with PVA. In the acidic pH range the deprotonated complex 110 is formed and its concentration reaches the

maximum percentage (98%) at  $\text{pH} \approx 8$ , whereas, the deprotonated complex species 120 starts to form at  $\text{pH} \approx 7.8$  and reaches its maximum percentage (60%) starting from  $\text{pH} 10$ .

Fig. 4 presents the visible spectra scanned for the binary Cu (II) complexes with PVA. The aquated copper (II) ion (mixture A) shows a broad, weak band with a maximum wavelength at 817 nm being attributed to the  $2T_{2g} \leftarrow 2E_g$  transition [3]. The binary  $[\text{Cu}(\text{PVA})_2]$  complex (mixture B) shows an absorption maximum at  $\approx 640$  nm. This shift in the absorption spectrum towards shorter wavelength (blue shift) is an evidence of the binary complex formation together with the potentiometric measurements.

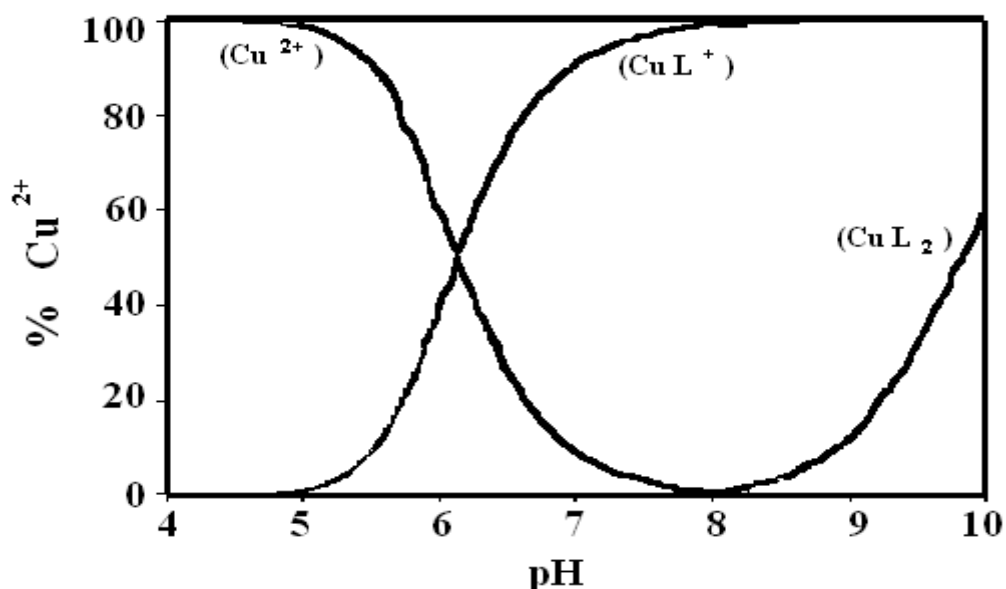


**Figure 3.** Concentration distribution diagram of the various forms of Cu(II).

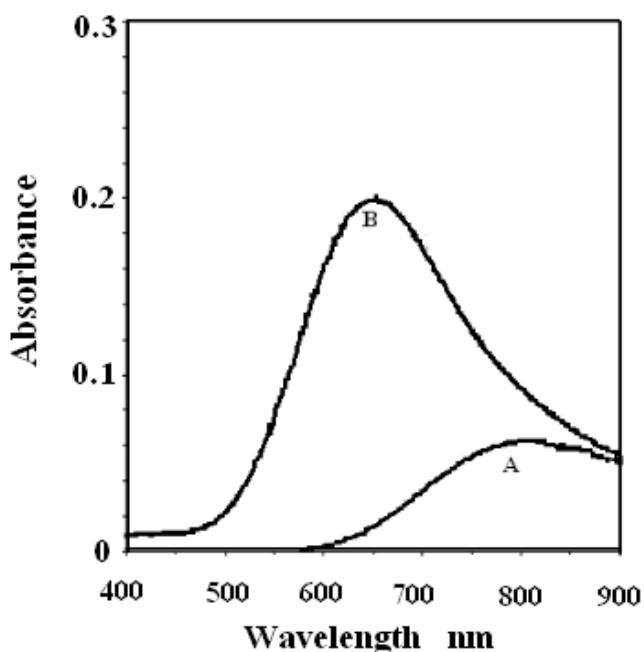


**Figure 4.** Visible spectra of [Cu-PVA] system. Curves: A: Cu(II); B: [Cu-PVA]

### 3.3. Relationships between the properties of central metal ions and stability constants of complexes

The relationships between the properties of the studied central metal ions and the stability constants of their complexes were discussed in an effort to give information about the nature of chemical bonding in complexes and make possible the calculation of unknown stability constants. Fig 5. Displays graphically the stability order of the complex forming ability of the transition metal ions. From Fig. 5 it could be seen that  $\log K_1$  values are arranged in the order  $\text{Co} < \text{Ni} < \text{Cu} > \text{Zn}$ . This stability order is in accordance with Irving- William's order [22,23] for divalent metals of 3d series. The extra stability of Cu(II) complex could be attributed to the Jahn - Teller effect. It was reported that the stability constants for complexes of metal ions of the same charge is inversely proportional to metal ion radii<sup>[24-25]</sup>, based on the electrostatic interaction between the metal ion and the ligand. This relationship may be approximately valued for ions of similar electronic configuration. Fig. 5a shows a linear plot of  $\log K_1$  of the

metal chelates of the ligand against the reciprocal ionic radii  $R$ . The corresponding data are presented in Table 3. Plotting  $\log K_1$  values against electronegativity of metal atoms give more or less straight line as shown in Fig. 5b. This may be explained on the basis that when the electronegativity difference between a metal atom and a ligand decreases, as a result of increasing the electronegativity of the metals, the covalent character of the metal-ligand bond would increase which in turn result into higher stability of the metal chelates. Fig. 5c shows the relationship between  $\log K_1$  values and the second ionization potential of the studied bivalent metal ions. A more or less straight line is obtained which is in accordance with the Van Panthaleon- Van Ech Eq. 5[24].

$$\text{Log } k_1 = P(I-q) \quad (5)$$

Where,  $I$  represent the ionization potential for the reaction ( $M \rightarrow M^{m+} + me$ ) in the gaseous phase,  $P$ ,  $q$  are constants independent of the metal ion but depends on the experimental conditions and the nature of ligand.  $P$  depends on the number of the donor groups of the ligand and  $q$  is the number of electrons involved in complex formation.

**Table 3.** Atomic number, ionic radius, electronegativity and ionization potential of the investigated bivalent metal ion(25).

| Metal ion  | $\text{Cu}^{2+}$ | $\text{Co}^{2+}$ | $\text{Ni}^{2+}$ | $\text{Zn}^{2+}$ |
|--|------------------|------------------|------------------|------------------|
| Atomic number  | 29               | 27               | 28               | 30               |
| Ionic radius( $R.A^0$ )                              | 0.71             | 0.79             | 0.72             | 0.74             |
| Electronegativity(E. N)                              | 2.00             | 1.88             | 1.91             | 1.65             |
| Second ionization potential( $\text{K J mol}^{-1}$ ) | 1968             | 1648             | 1753             | 1733.3           |

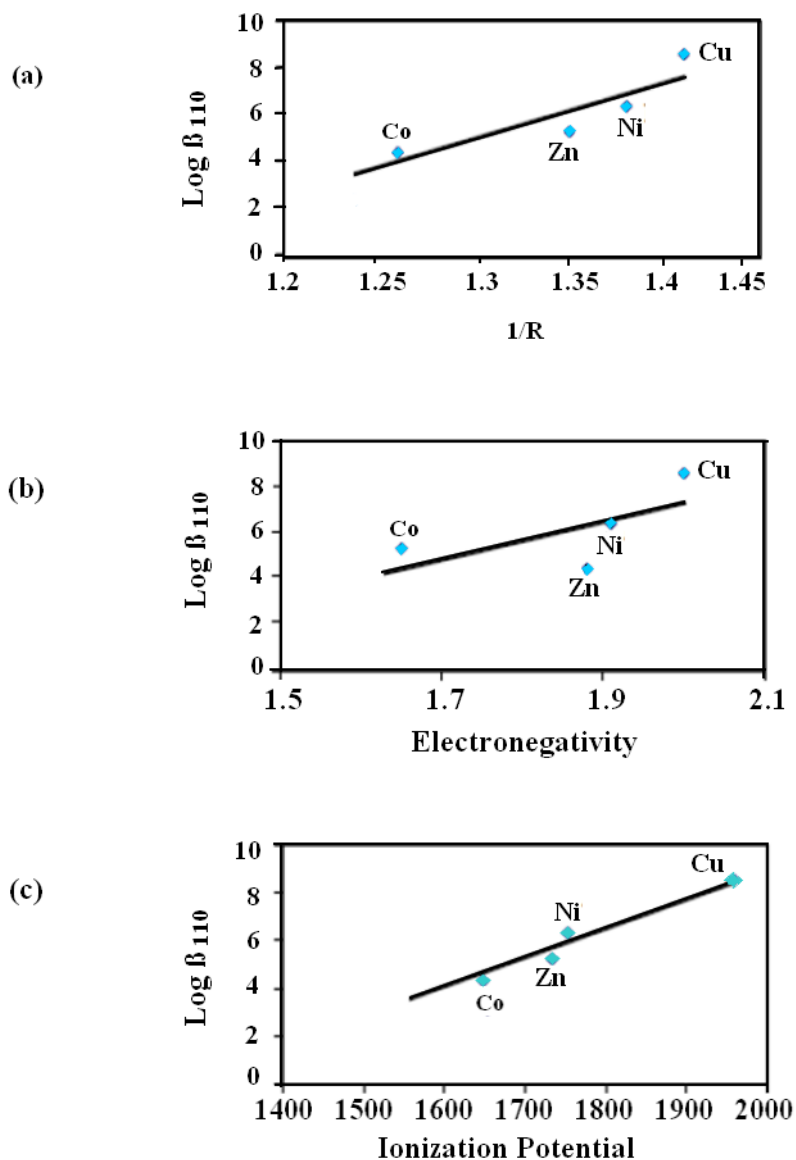


**Figure 5.** Effect of metal ion properties on the stability constant of PVA-complexes.

#### 4. ANTIMICROBIAL ACTIVITY

The PVA ligand is biologically active and its activity may arise from the hydroxyl groups which may play an important role in the antibacterial activity<sup>[26]</sup>. To assess the biological potential of the synthesized compounds, the PVA ligand and its metal complexes were tested against the selected bacteria and fungi (Fig. 6). The antimicrobial data were collected in Tables 4 and 5. The synthesized compounds were found to be more toxic compared with their parent PVA ligand against the same micro-organism and under the identical experimental conditions.

The increase in biological activity of the metal chelates may be due to the effect of the metal ion on the normal cell process. A possible mode of toxicity increase may be considered in the light of Tweedy’s chelation theory [27]. Chelation considerably reduce the polarity of the metal ion because of partial sharing of its positive charge with the donor group and possible p-electron delocalization within the whole chelate ring system that is formed during coordination. Such chelation could enhance the lipophilic character of the central metal atom and hence increasing the hydrophobic character and lipo solubility of the complex favoring its permeation through the lipid layers of the cell membrane. This enhances the rate of uptake/entrance and thus the antimicrobial activity of the testing compounds. Accordingly, the antimicrobial activity of the three complexes can be referred to the increase of their lipophilic character which in turn deactivates enzymes responsible for respiration processes and probably other cellular enzymes, which play a vital role in various metabolic pathways of the tested microorganisms. The antibacterial activity can be ordered as  $[Cu(PVA)] > [Ni(PVA)]$ , suggesting that the lipophilic behavior increases in the same order. The results indicate that, the two complexes exhibited moderate activity against the fungal strains when compared with standard Amphotericin. The tested complexes were more active against Gram-positive than Gram-negative bacteria, it may be concluded that the antimicrobial activity of the compounds is related to cell wall structure of the bacteria. It is possible because the cell wall is essential to the survival of bacteria and some antibiotics are able to kill bacteria by inhibiting a step in the synthesis of peptidoglycan.

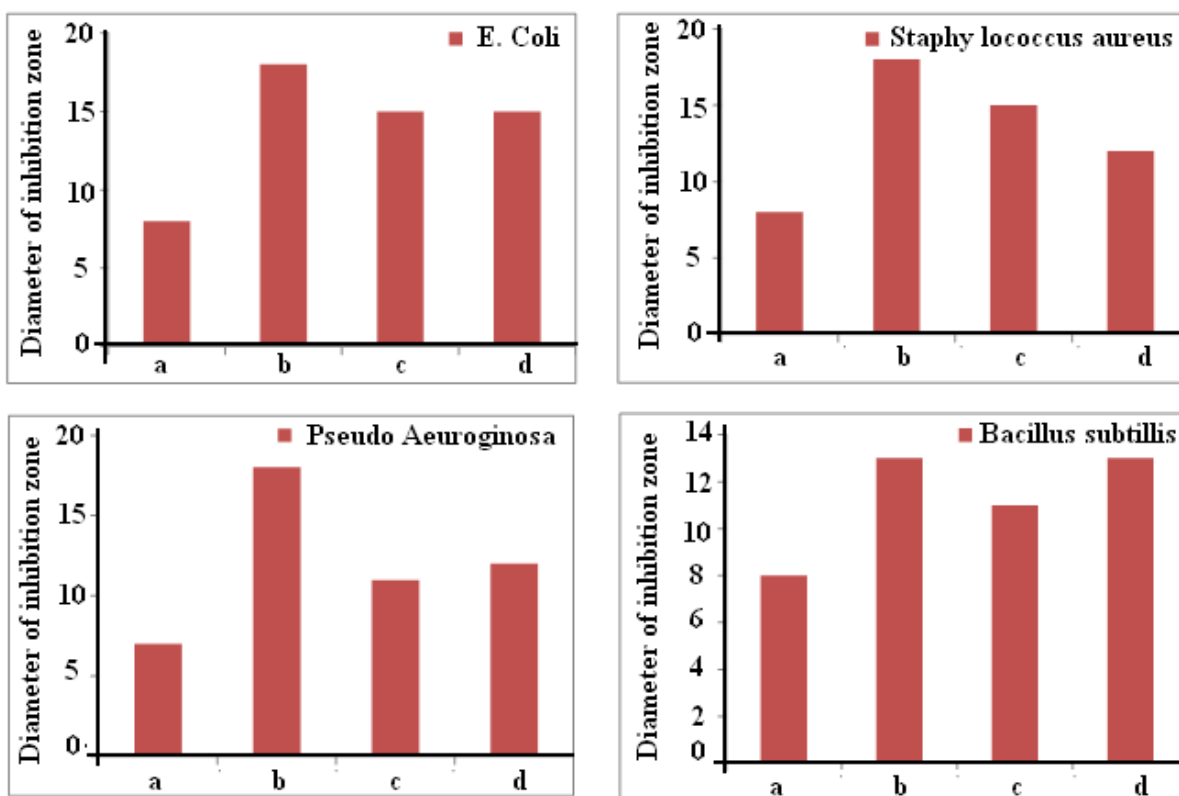


**Figure 6 .** Biological activity of metal complexes towards different types of bacterial strains where a: L, b:  $[CuL.2H_2O]2H_2O$ , c: $[NiL.4H_2O]2H_2O$ , d: Ampicilin

**Table 4** Antibacterial activity of the isolated complexes

| Complex                  | Gram Positive                |     |    |                          |     |    | Gram Negative                  |     |    |                         |     |    |
|--------------------------|------------------------------|-----|----|--------------------------|-----|----|--------------------------------|-----|----|-------------------------|-----|----|
|                          | <i>Staphylococcus aureus</i> |     |    | <i>Bacillus subtilis</i> |     |    | <i>Pseudomonas aereuginosa</i> |     |    | <i>Escherichia coli</i> |     |    |
| C (mg ml <sup>-1</sup> ) | 1                            | 2.5 | 5  | 1                        | 2.5 | 5  | 1                              | 2.5 | 5  | 1                       | 2.5 | 5  |
| PVA                      | -                            | 9   | 8  | -                        | 9   | 8  | -                              | 9   | 7  | -                       | 9   | 8  |
| CuL.2H <sub>2</sub> O    | 9                            | 13  | 18 | -                        | 10  | 13 | 10                             | 15  | 18 | 10                      | 14  | 18 |
| NiL.4H <sub>2</sub> O    | -                            | 12  | 15 | -                        | 10  | 11 | -                              | 10  | 11 | 10                      | 12  | 15 |
| Ampicillin (standard)    | -                            | 12  | 12 | -                        | 11  | 13 | -                              | 0   | 12 | -                       | 13  | 15 |

**Table 5.** Antifungal activity of the PVA ligand and its metal complexes

| Ligand/Complex          | Fungi                     |                         |
|-------------------------|---------------------------|-------------------------|
|                         | <i>Aspergillus flavus</i> | <i>Candida albicans</i> |
| PVA                     | 12                        | 12                      |
| CuL.2H <sub>2</sub> O   | 15                        | 16                      |
| NiL.4H <sub>2</sub> O   | 14                        | 15                      |
| Amphotericin (standard) | 17                        | 17                      |

Gram-positive bacteria possess a thick cell wall containing many layers of peptidoglycan and teichoic acids, but in contrast, Gram negative bacteria have a relatively thin cell wall consisting of a few layers of peptidoglycan surrounded by a second lipid membrane containing lipopolysaccharides and lipoproteins. These differences in cell wall structure can produce differences in antibacterial susceptibility and some antibiotics can kill only Gram-positive bacteria and is infective against Gram-negative pathogens<sup>[28]</sup>. Structure activity relationships evidence that the complexation with copper enhances the antimicrobial activity of the ligands against some of the tested organisms. Since copper chelates have an enhanced antimicrobial activity, in comparison to their analogous containing nickel(II) ions, the metal seems to play a relevant role in the activity of these compounds. These results may be due to higher stability constant of the Cu(II) complexes than the Ni(II) complexes (Table 2).

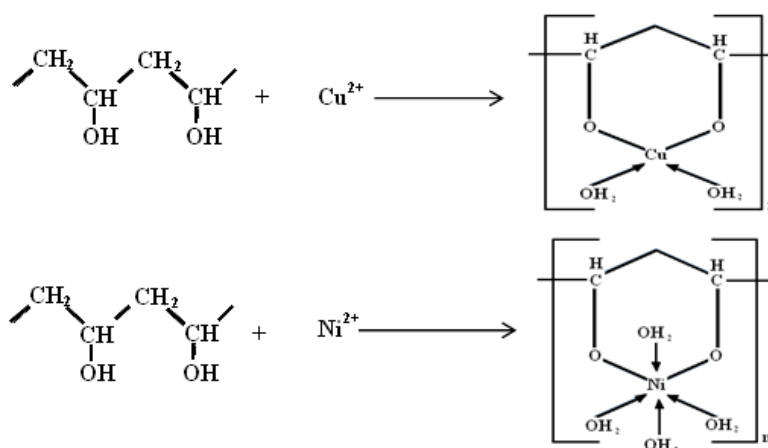
## 5. INFRA RED, ELECTRONIC SPECTRA AND MAGNETIC MEASUREMENTS

The study of the spectral and magnetic properties of the solid complexes provides information that can throw considerable light on their geometry. The analytical data show that the ligand forms 1:1

complex with Cu(II) and Ni(II). Generally, it is difficult to use infrared spectroscopy to fully elucidate the structure of complexes. However, it can provide some useful information on the functional groups of the ligand chelated with metal ions, especially with metal complexes of hydroxyl groups [29, 30]. The IR spectrum of the ligand and its complexes show bands in the region 4000-3000  $\text{cm}^{-1}$  in addition to band occurring at 2922  $\text{cm}^{-1}$  and 1124  $\text{cm}^{-1}$ , characteristic of hydrogen bonded O-H stretching [31-33] and antisymmetric stretching vibrations of both  $\text{CH}_2$  and COC respectively. On the other hand, for PVA cross-linked by  $\text{Cu}^{\text{II}}$  and  $\text{Ni}^{\text{II}}$  the band maximum corresponding to bonded OH group (3430  $\text{cm}^{-1}$ ), was shifted to lower frequencies; 3377  $\text{cm}^{-1}$  and 3384  $\text{cm}^{-1}$ , respectively. This indicates that hydroxyl groups were involved in chelation [34]. The antisymmetric stretching vibration ( $\nu$ )  $\text{CH}_2$  (2922  $\text{cm}^{-1}$ ), of cross-linked PVA became narrow compared with the non-cross-linked PVA and its complex with  $\text{Ni}^{\text{II}}$  and  $\text{Cu}^{\text{II}}$ . This is also supported by the appearance of new bands at 520-530  $\text{cm}^{-1}$  in the spectra of complexes, which were not found in the spectrum of the free ligand, possibly assignable to  $\nu$  M-O stretching vibration. The structures of the isolated solid complexes are proposed on the basis of the spectral and magnetic studies. The electronic spectrum of the Cu (II) complex gives a broad band with a maximum at 14211  $\text{cm}^{-1}$ , in consistence with that reported for square planer geometry [35]. The square planer geometry for the Cu(II) complex is also supported by calculating the room temperature magnetic moment. The electronic spectra of Cu(II)-PVA complex consists of a broad band in the 13500-16000  $\text{cm}^{-1}$  range is thought to originate from L  $\rightarrow$  M charge transfer [36]. The Cu (PVA) complex has magnetic moment value of 1.95, Table 1, provide additional evidence for the approximate square configuration [37-39]. The electronic spectra of the Ni(II)-PVA complex show two main absorption bands at the quite similar position in the visible region, as generally observed for high spin octahedral nickel(II) complex, and are assigned to  ${}^3\text{A}_{2g} \rightarrow {}^3\text{T}_{1g}(\text{F})$  and  ${}^3\text{A}_{2g} \rightarrow {}^3\text{T}_{2g}$  transitions, respectively. The  ${}^3\text{A}_{2g} \rightarrow {}^3\text{T}_{1g}(\text{P})$  transition in the polymer complex is also observed, furthermore, the magnetic moments lie in the range reported for this geometry [40,41].

From all results discussed above, the structural of the isolated complexes may be given as the following in scheme 1.

Further investigation to provide more convincing evidence for the structure of these complexes requires further studies including, e.g., X-ray diffraction studies and other structural investigation.



**Scheme.1.** Structure of PVA ligand and its metal complexes M (II)

## 6. CONCLUSION

The present work describes the acid-base equilibria of polyvinyl alcohol abbreviated as (PVA), and the complex formation equilibria with the metal ions Cu<sup>(II)</sup>, Ni<sup>(II)</sup>, Co<sup>(II)</sup>, and Zn<sup>(II)</sup>, to ascertain the composition and stability constants of the complexes. The results showed that the stability of the complexes can be ordered as Co (PVA) < Ni (PVA) < Cu (PVA) > Zn (PVA). The effect of metal ion properties on the stability of the complexes was investigated. Some solid complexes were synthesized and characterized. Their structures and formation are determined using microanalysis, magnetic, and different spectral tools. The Stoichiometry and stability constants of the complexes formed are reported at 25°C and 0.1 M ionic strength. The results show the formation of 1:1 and 1:2 complexes. The concentration distribution diagrams of the complexes were evaluated. It would be possible to calculate the equilibrium distribution of the metal species in biological fluids where all types of ligands are present simultaneously. The antibacterial activity results indicated that tested complexes were more active against the selected types of bacteria than the free PVA ligand. The antibacterial activity of the isolated metal chelates obeyed this order [Cu(PVA)] > [Ni (PVA)] which is in accordance with the stability constants order  $\log K_{Cu-PVA} = 8.07 > \log K_{Ni-PVA} = 6.21$

## References

1. S.M. Burkinshaw, N.A. Kumar, *Dyes and Pigments* 77 (2008) 86-91.
2. N. Hojo, H. Shirai, S. Hayashi, *J. Polym. Sci. Polym. Symp.* 47 (1974) 299-307.
3. A.A. Shoukry, W.M. Hosny, *Cen. Eur. J. Chem.* 10 (2012) 59-70.
4. C. Vasile, A.K. Kulshreshtha, *Handbook of Polymer Blends and Composites*, Rapra Technology. Ltd.: Shawbury, UK, 2003, pp. 288–365.
5. B. Ratner, A.S. Hoffman, F.J. Schoen, J.E. Lemons, *Biomaterials science: An introduction to materials in medicine*, Elsevier Academic Press, San Diego, 2004.
6. C.M. Hassan, N.A. Peppas, *Adv. Polym. Sci.* 153 (2000) 37–65.
7. J.H. Chen, L. Hwang, *J. Chin. Chem. Soc.* 35 (1988) 273-281.
8. W.M. Hosny, A.K. Abdel Hadi, H. El-Said, A.H. Basta, *Polym. Int.* (1995) 37, 93.
9. A.H. Basta, W.M. Hosny, *Polym. Deg. and Stab.*, 60 (1998) 239-245.
10. W.M. Hosny, A.H. Basta, H. El-Said, *Polym. Int.* 42 (1997) 157-162.
11. W.M. Hosny, S. M. El-Medani, M.M. Shoukry, *Talanta* 48 (1999) 913-921.
12. Vogel's Text Book of Quantitative chemical analysis, fifth ed., Longman, UK, 1989, Ch. 10, pp. 326.
13. A.W. Bauer, W.M. Kirby, C. Sherris, M. Truck, *J. Am. Clin. Path.* 45 (1966) 493–496.
14. M.A. Pfaller, L. Burmeister, M.A. Bartlett, M.C. Rinaldi, *J. Clin. Microbiol.* 26 (1988) 1437-1441.
15. National Committee for Clinical Laboratory Standards (1993), *Methods for dilution antimicrobial susceptibility tests for bacteria that grow aerobically*, third ed., Approved standard M7- A3. NCCLS, Villanova, Pa.
16. L. D. Liebowitz, H. R. Ashbee, E. G. V. Evans, Y. Chong, N. Mallatova, M. Zaidi, D. Gibbs, *Elsevier* 27 (2001) 24.
17. Matar, M.J; Ostrosky-Zeichner, L; Paetznick, V. L; Rodriguez, E. Chen; Rex, J.H, *Antimicrob. Agents Chemother.* 47 (2003) 1647-1651.
18. J. Stark, H.G. Wallace, *Chemistry Data Book*, Murray, London, 1975, pp. 75.
19. R.J. Angelici, *Synthesis and Technique in Inorganic Chemistry*, second ed., W.B. Saunders Company, Philadelphia, 1977, pp. 198.

20. P. Gans, A. Sabatini, A. Vacca, *J. Inorg. Chim. Acta* 18 (1976) 237-239.
21. M.M. Shoukry, A.A. Shoukry, P.A. Khalf Allas, S. S. Hassan, *Int. J. Chem. Kinet.* 42 (2010) 608-618.
22. (a) H. Irving, R. J. P. Williams, *Nature* 162 (1984) 746,  
(b) H. Irving, R. J. P. Williams, *J. Chem. Soc.*, 1953, 3192-3210.
23. F.A. Cotton, G. Wilkinson, *Advanced Inorganic Chemistry*, Wiley & Sons, New York, 1962.
24. M.T. Beck, *Chemistry of Complex Equilibria*, Van Nostrand Reinhold Co., London, 1962.
25. J. E. Huheey, *Inorganic chemistry-Principles of Structure and Reactivity*, Harper and Row, New York, 1983.
26. N. Sari, S. Arslan, E. Logoglu, I. Sakiyan, *G.U. J. Sci.* 16 (2003) 283-288.
27. B.G. Tweedy, *Phytopathology* 55 (1964) 910-914.
28. A.L. Koch, *Clin. Microbiol. Rev.* 16 (2003) 673-687.
29. L.G. Tang, D.N.S. Hon, *J. App. Polym. Sci.* 29 (2000) 1476-1485.
30. M.Melnik, *Coord. Chem. Rev.* 36 (1981) 1-44
31. Z.M. Zaki, G.G. Mohamed, *Spectrochimica Acta- Part A* 26 (2000) 1245-1250.
32. J.B. Gandhi, N.D. Kulkarni, *Polyhedron* 18 (1999) 1735-1742.
33. A. Soliman, W. Linert, *Thermochimica.Acta* 338 (1999) 67-75
34. A.A. Shoukry, M.M. Shoukry, *Spectrochimica Acta* 70 (2008) 686-691.
35. A.A. Soliman, G.G. Mohamed, W.M. Hosny, M.M. El-Mawgood, *J. Synth. React. Inorg. Met-org. and Nano-Metal Chem.* 35 (2005) 483-490.
36. R.G. Bates, *Determination of pH Theory and Practice*, second ed., Wiley interscience, New York, 1975.
37. M.F. Iskander, T.E. Khalil, R. Waase, W. Haase, I. Savoboda, H. Fuess, *Polyhedron* 19 (2000) 949-958.
38. M. Palaniandavar, C. Natarajan, *Aust. J. Chem.* 33 (1980) 737-745.
39. J. Vanco, J. Marek, Z. Travnicek, E. Racanska, J. Muselik, O. Svajlenova, *J. Inorg. Biochem.* 102 (2008) 595-605.
40. B.P. Lever, *Inorganic Electronic spectroscopy*; Elsevier, Amsterdam, 1968.
41. Jorgensen, C.K, *Absorption Spectra and Chemical Bonding Complexes*, Pergemon Press. Oxford, 1964, pp. 206.